

2011

High-sensitivity detector for molecular sensing using magnetic particles

Damien Le Roy

University of Nebraska-Lincoln, damien.le-roy@grenoble.cnrs.fr

W. Yang

Nebraska Center for Materials and Nanoscience

X. Yin

Nebraska Center for Materials and Nanoscience

R. Y. Lai

Nebraska Center for Materials and Nanoscience, rlai2@unl.edu

Sy_Hwang Liou

University of Nebraska-Lincoln, sliou@unl.edu

See next page for additional authors

Follow this and additional works at: <http://digitalcommons.unl.edu/physicsellmyer>

Le Roy, Damien; Yang, W.; Yin, X.; Lai, R. Y.; Liou, Sy_Hwang; and Sellmyer, David J., "High-sensitivity detector for molecular sensing using magnetic particles" (2011). *David Sellmyer Publications*. 247.
<http://digitalcommons.unl.edu/physicsellmyer/247>

This Article is brought to you for free and open access by the Research Papers in Physics and Astronomy at DigitalCommons@University of Nebraska - Lincoln. It has been accepted for inclusion in David Sellmyer Publications by an authorized administrator of DigitalCommons@University of Nebraska - Lincoln.

Authors

Damien Le Roy, W. Yang, X. Yin, R. Y. Lai, Sy_Hwang Liou, and David J. Sellmyer

High-sensitivity detector for molecular sensing using magnetic particles

D. Le Roy,^{1,2,a)} W. Yang,^{1,3} X. Yin,^{1,2} R. Y. Lai,^{1,3} S.-H. Liou,^{1,2} and D. J. Sellmyer^{1,2}

¹Nebraska Center for Materials and Nanoscience, Lincoln, Nebraska 68588, USA

²Department of Physics and Astronomy, University of Nebraska, Lincoln, Nebraska 68588, USA

³Department of Chemistry, University of Nebraska, Lincoln, Nebraska 68588, USA

(Presented 18 November 2010; received 23 September 2010; accepted 15 December 2010; published online 6 April 2011)

A scheme for molecular sensing using magnetic tracer particles and a microcantilever torsional magnetometer is investigated. The present report deals with the example of explosive 2,4,6-trinitrotoluene (TNT) detection. The sensors consist of silicon microcantilevers functionalized with TNT aptamers that are weakly bonded to magnetic particles via TNT-analog molecules. When exposed to TNT, the magnetic signal, initially maximum, is expected to undergo a steplike decrease as the TNT molecules replace the magnetic particles on the TNT receptors. We demonstrate the feasibility of this detection technique in terms of chemical reactions and our magnetometer sensitivity that reaches the range of 10^{-11} emu at room temperature with commercial atomic force microscopy cantilevers. © 2011 American Institute of Physics.

[doi:10.1063/1.3564951]

I. INTRODUCTION

The detection of potent explosive substances such as 2,4,6-trinitrotoluene (TNT) has been the scope of active research efforts during the past decade, as there are significant environmental and security needs. It yielded a broad array of schemes, from the direct gas phase analysis by means of ion-mobility spectrometry or IR spectroscopy techniques,¹ to receptor-based methods.²⁻⁴ A high sensitivity is needed especially because of the commonly low vapor pressure of those compounds² and sufficient selectivity to avoid unacceptable level of false alarms. In this regard, the use of chemical recognition molecules constitutes a promising way of improvement.⁵

Microcantilever-based resonators (MBR) were proved to enable the detection of attonewton forces.⁶ Subsequently, they have been used for different purposes, including *in situ* thickness measurement,⁷ nuclear moment resonance,⁸ or particles sensors based on mass detection, reaching the level of few femtograms.⁹⁻¹¹ Using a magnetic field excitation, MBR can be used as ultrasensitive magnetometers, with a record of sensitivity of $10^8 \mu_B$ at room temperature.^{8,12} Here we report on the use of this magnetometry technique to detect small amounts of TNT via tracer magnetic particles.

The detection process is represented in Fig. 1. It consists of three-steps: (a) the functionalization of the cantilevers with TNT aptamers, (b) the saturation of the receptors with magnetic tracer particles conjugated to TNT-analog molecules (DNP-NH₂), and (c) the exposure to TNT that triggers the desorption of the magnetic particles from the cantilever surface since the interaction between the aptamer and TNT is weaker than that between the aptamer and TNT. A steplike decrease of the magnetization proportional to the TNT concentration is then recorded. The feasibility of this

technique is demonstrated with regard to successful chemical reactions and the magnetic moment sensitivity of about 7.2×10^{-11} emu, which corresponds to the magnetic moment of a single Fe particle of 400 nm.

II. EXPERIMENTAL DETAILS

A diagram of the microcantilever torsional magnetometer (MTM) principle is displayed in Fig. 2(a). A magnetic particle is attached to the cantilever head. An external magnetic field H_0 aligns the particle magnetic moments along the y direction. An oscillating drive field H_t of 5 Oe amplitude is applied along the z direction. It exerts a magnetic torque τ on the cantilever along x that can be expressed as: $\tau = |\mu \times H_t|$ and simplified as: $\tau = \mu_0 m V H_T$ considering a small deflection, where m is the magnetic moment per unit volume, V , along the y direction. We assume that the magnetic torque leads to the cantilever neck bending, neglecting any bending in the

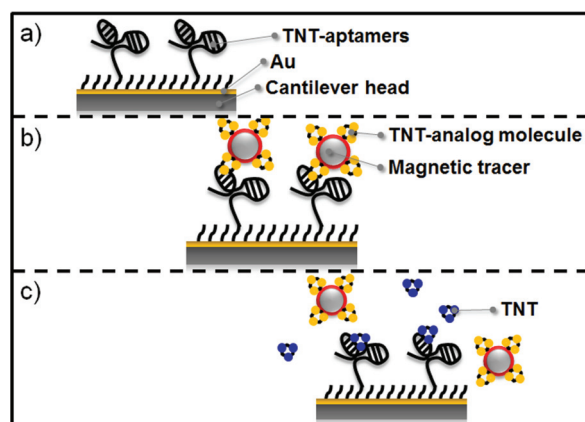


FIG. 1. (Color online) TNT detection principle. (a) TNT aptamers are immobilized on the Au-plated cantilever paddle (zero magnetization). (b) The TNT-analog-conjugated particles occupy the TNT receptors (maximum magnetization). (c) The TNT molecules replace the particles on the cantilever paddle (loss of magnetization).

^{a)}Author to whom correspondence should be addressed. Electronic mail: dleroy2@unlnotes.unl.edu.

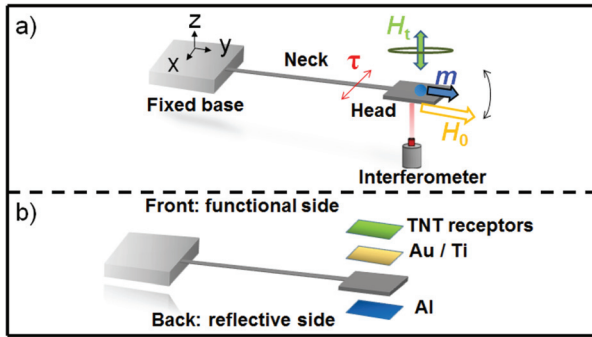


FIG. 2. (Color online) (a) Principle sketch of the magnetic detection by the MTM technique. (b) Upside coating of the cantilever head for chemical sensing. (c) Downside coating of the cantilever head for an increased reflectance.

fixed base. Considering a small paddle compared to the cantilever neck length, the displacement of the cantilever, Δz , can be expressed as:⁷

$$\Delta z = \frac{6\tau L_c^2}{Ew_c t_c^3} = \frac{6\mu_0 m H_T L_c^2}{Ew_c t_c^3}, \quad (1)$$

where L_c , w_c , t_c correspond to the dimensions of the cantilever neck, respectively, the length, the width, and the thickness, and E is the Young's modulus. The typical dimensions of the cantilevers considered here are $170 \mu\text{m} \times 7 \mu\text{m} \times 2 \mu\text{m}$ [Fig. 3(a)]. A magnetic particle with a moment of 1.7×10^{-11} emu would thus induce a deflection of 175 fm (for $H_T = 5$ Oe). By driving magnetically the cantilever bending at its natural frequency, f_0 (60 kHz), one increases the deflection by a factor Q (the quality factor of the resonator).

An interferometer is used to measure Δz . It includes an IR laser diode (AFM interferometer 0022-2000) of 5 mW power, with tunable wavelength between 1543.68 and 1547.83 nm. The interferometer cavity length z_0 is about $300 \mu\text{m}$, delimited by the end of the optical fiber and a cantilever side which is coated with a sputtered Al layer of 30 nm for better reflectance [see Fig. 3(b)]. The typical $V(\lambda)$ characteristic curves present oscillations of 3 V amplitude. The wavelength of the laser is adjusted in order to bias the Fabry–Perot cavity in the linear region of the transmission spectrum, where the voltage response to a wavelength change $\Delta V/\Delta\lambda$ is maximum, typically 1.5 V/nm. From the measurement of $\Delta V/\Delta\lambda$, one can translate a wavelength change into a displacement and subsequently a voltage change by:¹³

$$\frac{\Delta V}{V_0} = 4\pi v \left(\frac{\Delta z}{\lambda} - \varepsilon_0 \frac{\Delta\lambda}{\lambda^2} \right), \quad (2)$$

where V_0 is the bias voltage, v the fringe visibility [defined as $(V_{\text{max}} - V_{\text{min}})/(V_{\text{max}} + V_{\text{min}})$], and λ the wavelength. A noise level of $5 \mu\text{V}$ is generally observed, which corresponds to a minimum displacement detectable of 800 fm. The transmission spectrum is subjected to change from one measurement to the other, notably because of nonidentical alignments of the cantilever paddle with the optical fiber. Therefore it is recorded before each measurement, which enables us to accurately calibrate the magnetometer.

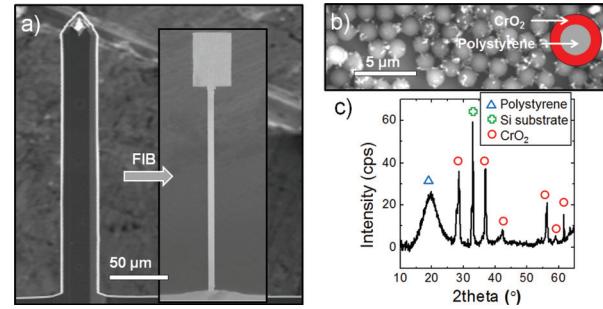


FIG. 3. (Color online) (a) SEM images of the cantilever before (left) and after (right) FIB milling. (b) SEM image of P@C particles lying on Si substrate. (c) X-Ray diffraction pattern measured on P@C particles assembly.

The sensitivity of the MTM technique also depends on the level of the cantilever thermal fluctuations. This noise can be expressed as an equivalent thermal noise per root hertz of:⁷ $\Delta z_{\text{min}} = \sqrt{2k_B T / \pi k Q f_0}$, where k is the spring constant, T the temperature, and k_B the Boltzmann constant. k can be either experimentally determined by force measurements or calculated in the case of a simple shape. For a bar bending at one end, k varies as: $w_c t_c^3 / 4l_c^3$.⁸ The microcantilevers are prepared from commercial silicon AFM cantilevers, by focused ion beam (FIB) milling [Fig. 3(a)]. The typical spring constant values we obtain are about 0.1 N/m, which corresponds to one order of magnitude less than the starting silicon cantilever. Because of cost efficiency restrictions for device application, we limit our investigations under moderate vacuum of 100 mTorr. The measured Q factor under magnetic excitation is 800. Considering the obtained values of k , Q , f_0 , and a typical lock-in amplifier measurement bandwidth of 3 Hz, the level of the thermal motion of the cantilever is around 40 fm.

As for the chemically active side of the cantilever, represented in Fig. 2(b), it is plated with a Ti (5 nm)/Au (40 nm) sputtered bilayer to ensure the adsorption of the thiol-terminated peptides. The thiol-terminated TNT-aptamer is purchased from Activotec (Cambridge, UK) and its sequence is as follows: (N terminus) WHWQRPLMPVSIK $(\text{CH}_2)_{11}$ -SH (C terminus). This sequence has been proved as a selective peptide aptamer for TNT over DNT and other analogs.¹⁴ The thiol terminated TNT aptamers are immobilized onto the gold-coated cantilevers by incubating cantilevers in $5 \mu\text{m}$ TNT-aptamer (acetate/acetic buffer, pH 5.0) for 1 h. The cantilevers are then rinsed with water and subsequently passivated with 2 mM 9-mercapto-1-nonanol ($\text{C}_9\text{-OH}$) overnight to displace nonspecifically bound aptamers. Polystyrene@CrO₂ particles (P@C) of $1.4 \mu\text{m}$ in diameter are supplied by Spherotec, Inc. (Lake Froest, IL) as an aqueous suspension of magnetic particles coated to provide free carboxyl groups. The SEM image displayed in Fig. 2(b) shows an assembly of the magnetic particles used in this study. The corresponding x-ray diffraction pattern of Fig. 2(c) shows an amorphous polystyrene core surrounded by a continuous CrO₂ shell that adopts the bulk tetragonal rutile structure. The particles are conjugated to DNP-NH₂, which serves as TNT-analog molecule. (DNP-NH₂, C₁₂H₁₈N₄O₄ · HCl) is synthesized according to the literature.¹⁵ DNP-NH₂ can be covalently attached to the carboxy-terminated particles with EDC/NHS reaction.¹⁶

III. RESULTS AND DISCUSSION

The magnetism of the TNT-analog conjugated P@C particles is first investigated on assembly using superconducting quantum interference device (SQUID) magnetometry at room temperature. The magnetization curve shows up an hysteresis below 1.5 kOe with a coercivity of 0.5 kOe and a saturated magnetization of 24 emu/cm^3 , reached for an applied field of 10 kOe. This corresponds to a maximum magnetic moment per particle of $3.4 \times 10^{-11} \text{ emu}$. For the sensor purpose, a fixed applied magnetic field would be sufficient. However, its magnitude should be in the reversible region and close to the saturation field in order to ensure similar and maximum magnetization loss when a particle leaves the sensor platform. Hence a field magnitude beyond 1.5 kOe would be desired, which is easily reached using common permanent magnets such as alnico or NdFeB. At 1.5 kOe, the magnetization is 50% of M_S , which results in a magnetic moment per particle of about $1.7 \times 10^{-11} \text{ emu}$. From the above-presented discussion and assuming identical magnetization among the particles, the magnetic moment of the overall assembly at 1 kOe is $3.2 \times 10^{-10} \text{ emu}$. Figure 4(b) displays successive magnetization curves of an assembly of 17 particles attached to the cantilever paddle, as shown on the SEM image of Fig. 4(a), and collecting an averaged signal over 20 points per field step. Doing so, the contribution of a single particle can be detected. From one magnetization curve to the other, one can find identical magnetization reversal steps, revealing the discrete amount of particles attached. It is remarked that the P@C particles have relatively small magnetization compared to particles made of pure 3d transition metals by more than one order of magnitude. Considering pure Fe, $7.2 \times 10^{-11} \text{ emu}$ corresponds to the magnetic signal of a spherical particle of 400 nm diameter.

In summary, we have described a novel technique for molecule sensing using MTM. It could be applied to any molecule if a combination peptide/analog can be found. The success of the involved chemical reactions between the explosive TNT with aptamer validates the principle of the method. From the analysis of the signal to noise ratio, we have reached a sensitivity of $7.2 \times 10^{-11} \text{ emu}$ at ambient temperature using a commercial atomic force microscopy cantilever that corresponds to the magnetic signal of a single Fe particle of 400 nm diameter. With further sensitivity improvements, notably obtained by thinning the cantilevers, a dual detection of the magnetization and the mass could be achieved by recording resonance frequency shifts. A single molecular detection under ambient conditions using this method would then be possible.

ACKNOWLEDGMENTS

The authors are grateful to Professor Dussault for his knowledgeable support. This work is supported by DOD

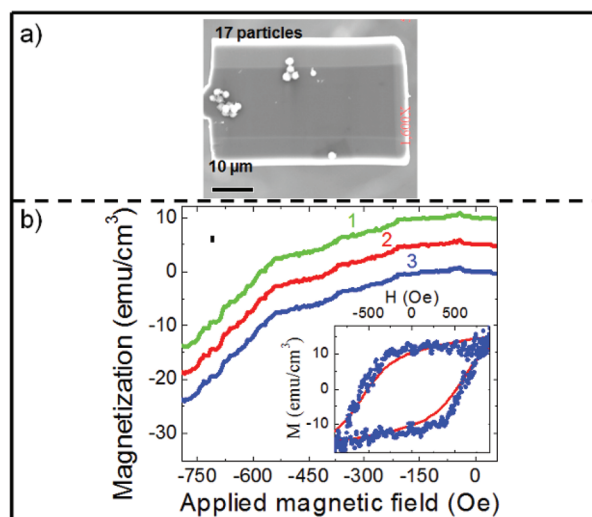


FIG. 4. (Color online) Top SEM image of P@C particles on the cantilever head. Bottom: corresponding successive magnetization curves, measured with MTM from positive applied field to negative. Curves 2 and 3 are voluntarily shifted downward for better clarity. The vertical bar on the top left represents the contribution of one particle in the magnetization reversal. The inset shows the entire hysteresis loop (circles) measured with MTM on the same particles assembly and a magnetization curve measured with a SQUID magnetometer on an assembly of around 10^8 particles.

(ARO) W911NF-08-1-01311, W911NF-09-2-0039, NSF MRSEC DMR-0820521, and Nebraska Center for Materials and Nanoscience.

¹M. B. Pushkarsky, I. G. Dunayevskiy, M. Prasanna, A. G. Tsekoun, R. Go, and C. K. N. Patel, *Proc. Natl. Acad. Sci. U.S.A.* **103**, 19630 (2006).

²L. Senesacand and T. G. Thundat, *Mater. Today* **11**, 28 (2008).

³S. Tao and G. Li, *Colloid. Polym. Sci.* **285**, 721 (2007).

⁴S. Dohn, W. Svendsen, A. Boisen, and O. Hansen, *Rev. Sci. Instrum.* **78**, 103303 (2007).

⁵Z. Kuang, S. N. Kim, W. J. Crookes-Goodson, B. L. Farmer, and R. R. Naik, *ACS Nano* **4**, 452 (2010).

⁶T. D. Stowe, K. Yasumura, T. W. Kenny, D. Botkin, K. Wago, and D. Rugar, *Appl. Phys. Lett.* **71**, 288 (1997).

⁷J. Moreland, J. A. Beall, and S. E. Russek, *J. Magn. Magn. Mater.* **242-245**, 1157 (2002).

⁸M. D. Chabot, J. M. Moreland, L. Gao, S.-H. Liou, and C. W. Miller, *J. Microelectromech. Syst.* **14**, 1118 (2005).

⁹S. Dohn, S. Schmid, F. Amiot, and A. Boisen, *Appl. Phys. Lett.* **97**, 044103 (2010).

¹⁰T. H. Stievater, W. S. Rabinovich, M. S. Ferraro, N. A. Papanicolaou, J. B. Boos, R. A. McGill, J. L. Stepnowski, and E. J. Houser, *Appl. Phys. Lett.* **89**, 091125 (2003).

¹¹N. V. Lavrik and P. G. Datskos, *Appl. Phys. Lett.* **82**, 2697 (2003).

¹²J. P. Davis, D. Vick, D. C. Fortin, J. A. J. Burgess, W. K. Hiebert, and M. R. Freeman, *Appl. Phys. Lett.* **96**, 072513 (2010).

¹³K. J. Bruland, J. L. Garbini, W. M. Dougherty, S. H. Chao, S. E. Jensen, and J. A. Sidles, *Rev. Sci. Instrum.* **70**, 3542 (1999).

¹⁴J. W. Jaworski, D. Raorane, J. H. Huh, A. Majumdar, and S.-W. Lee, *Langmuir* **24**, 4938 (2008).

¹⁵C. G. Knight and N. M. Green, *Biochem. J.* **159**, 323 (1976).

¹⁶EDC: 1-Ethyl-3-(3-dimethylaminopropyl) carbodiimide, NHS: N-Hydroxysuccinimide.